First Principles Studies of the Effect of Ostwald Ripening on Carbon Nanotube Chirality Distributions

Anders Börjesson[†,‡] and Kim Bolton[†]

[†]University of Borås, SE-501 90 Borås, Sweden and [‡]University of Gothenburg, SE-412 96 Gothenburg, Sweden

ABSTRACT The effect of Ostwald ripening of metal particles attached to carbon nanotubes has been studied using density functional theory. It has been confirmed that Ostwald ripening may be responsible for the termination of growth of carbon nanotube forests. It was seen that the Ostwald ripening of metal particles attached to carbon nanotubes is governed by a critical factor that depends on both the cluster size and the carbon nanotube chirality. For example, clusters attached to armchair and zigzag nanotubes of similar diameters will have different critical factors although the exact behavior may depend on which molecules are present in the surrounding medium. The critical factor was also observed to have a critical point with the effect that clusters with a narrow size distribution close to the critical point may experience a narrowing rather than a widening of the size distribution, as is the case for free clusters.

KEYWORDS: carbon nanotube growth · Ni nanoparticle · density functional theory · molecular dynamics · Ostwald ripening

Controlled growth of carbon nanotubes (CNTs) is vital for the full scale realization of many proposed CNT-based applications such as nanoelectronics,[1,2] electrochemical capacitors,[3] reinforcements in polymer composites,[4,5] and additives for electrically[6] and thermally[7] conducting composites. For example, a recent report by Ci *et al.*[8] shows that composites with long carbon nanotubes allow for maximal utilization of the high modulus and strength of CNTs and that directionally aligned CNTs are desirable compared to randomly dispersed CNTs of the same length. It has also been observed that a composite with directionally aligned CNTs shows different conductance behavior than a composite with randomly aligned CNTs[9] and that the conductance is anisotropic and depends on the orientation of the CNTs.

Chemical vapor deposition (CVD) is the most successful method for production of long, directionally aligned CNTs.[10,11] For this method to be fully applicable for systematic production of CNTs, it is important to understand which parameters control the quality and length of the CNTs produced. It has been discussed that the growth rate may be limited by the diffusion rate of the carbon feedstock[12] as well as the diffusion rates of carbon in[11] and on[13] the catalyst particle. It has also been suggested that the formation of carbon structures on the catalyst surface will poison the catalyst particle and serve as a limiting factor[14] of the growth process.

It has been shown that water-assisted CVD growth[15,16] (supergrowth) is an efficient method to delay the poisoning of the catalyst particle and that it allows for growth of dense millimeter-long CNT forests. Although supergrowth has led to a significant advance, the lifetime and activity of catalyst particles are still limiting the yield. Recent reports suggest that the presence of water in the growth chamber may also inhibit the process of Ostwald ripening of the catalyst particles,[17] hence reducing the increase in the number of larger particles at the expense of smaller ones. It has also been discussed that catalyst deactivation is due to a combination of Ostwald ripening and diffusion of the catalyst particles into the substrate material.[18] It was shown that the rates of subsurface diffusion and Ostwald ripening for Fe catalysts of diameters of a few nanometers were dependent on the method of production and porosity of the substrate.[19]

Ostwald ripening[20,21] is a process where a system of particles seeks to increase the system's global stability by increasing the particle bulk-to-surface fraction, that is, increasing the volume and decreasing the surface area. This is due to the higher energy of surface atoms compared to the bulk atoms, and the result is that smaller clusters, below a critical size, will decrease in size, and larger clusters, above the critical size, will increase their size. For free clusters the critical size is equal to the average size of the distribution.[22]

*Address correspondence to anders.borjesson@hb.se.

Received for review May 31, 2010 and accepted January 14, 2011.

Published online January 31, 2011
10.1021/nn101214v

To understand the mechanisms of CNT growth termination due to Ostwald ripening, it is of great relevance to know whether there is a difference in the ripening rate of catalysts attached to CNTs of different chirality. This intricate issue is addressed by first principles density functional theory (DFT) calculations. The same DFT methods used here have previously been used to provide useful information about CNT−metal systems. For example, it has been shown the metal adapts its shape to the CNT and not *vice versa*,[23] that the adhesion energy between zigzag CNTs and metal is significantly stronger than the adhesion between armchair CNTs and metal[24,25] while the adhesion between CNTs and metal-carbides is similar to that of the CNT and pure metal particles.[25]

The analysis presented here is mainly based on comparisons of total energies of sets containing an equal number of C, Ni, and H atoms. Typically, these sets contain two CNTs, possibly with different chirality, either attached to Ni clusters or having an open end. In the figures presented below, the relative energy between two sets are given. This relative energy is defined as the energy difference between a set with two identical CNT−metal systems and a set with one open-ended CNT and all metal atoms on the other CNT, that is, $E_{rel} = 2 \times E_{CNT-Ni_x} - E_{CNT-Ni_{2x}} - E_{CNT}$. A positive relative energy indicates that the set with a large cluster is favored over the set with two small clusters.

To study the stability of individual atoms in the cluster, the atomic energy of atom i is defined as

$$E_i^{atomic} = E_N - E_{N-i} \quad (1)$$

where E_N is the total energy of a system N and E_{N-i} is the total energy of the same system but with atom i excluded (*i.e.*, the cluster with atom i removed is not relaxed). The atomic energies for all Ni atoms have been calculated for some atomic geometries and allow for direct comparison of relative stability between atoms within the same structure. Since the clusters with $N - 1$ atoms are not relaxed after removal of the atom, these energies provide no information about the diffusion rates or mechanism of individual atoms but rather which atoms are most thermodynamically stable.

Ni atoms have been characterized into the categories bulk, surface, and interfacial depending on their coordination numbers. The coordination number of Ni atom i is calculated according to

$$f(r, R_1, R_2) = \begin{cases} 1 & r \le R_1 \\ \left(1 + \cos\left(\frac{r - R_1}{R_2 - R_1}\pi\right)\right)/2 & R_1 < r \le R_2 \\ 0 & r > R_2 \end{cases}$$

$$\text{coord}_{Ni-Ni,\,i} = \sum_{j \neq i} f(r_{i,j}, R_1, R_2) \quad (2)$$

$$\text{coord}_{Ni-C,\,i} = \sum_{k} f(r_{i,k}, R_1, R_2) \quad (3)$$

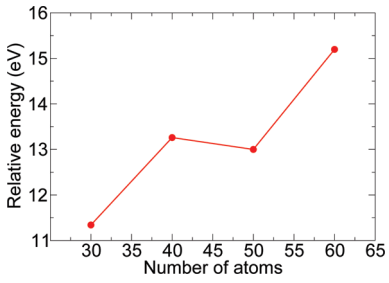

Figure 1. The relative energy between sets containing two free Ni_x clusters and one Ni_{2x} cluster as a function of the total number of atoms. All sizes have a positive relative energy indicating that even at the nanoscale the larger clusters are energetically more favorable than two smaller clusters.

where the summation is over all Ni (eq 2) and C (eq 3) atoms, respectively, $r_{i,j}$ is the distance between Ni atoms i and atom j, and $r_{i,k}$ is the distance between Ni atom i and C atom k. The parameters are $R_1 = 2.7$ Å and $R_2 = 3.2$ Å for the Ni−Ni coordination numbers and $R_1 = 2.7$ Å and $R_2 = 3.0$ Å for the Ni−C coordination numbers. This procedure and parameters were successfully used in the construction of a many-body potential for Ni and C.[26]

RESULTS AND DISCUSSION

The smallest number of particles that can experience Ostwald ripening is two, where the smallest particle will decrease in size in favor of the larger one. Free Ni clusters are initially examined in order to understand whether nanoscaled Ni clusters will experience Ostwald ripening. Figure 1 shows the relative energies of sets containing 30, 40, 50, and 60 Ni atoms, distributed as either one large cluster or two smaller clusters of the same size. All systems have a positive relative energy, showing that the set with one large cluster is more stable than the set with two small clusters. That is, Ostwald ripening occurs as soon as there exists a size difference between the clusters.

The situation is similar when the clusters are attached to CNT ends, except for the presence of the adhesion energy between the CNTs and the Ni clusters. Diffusion of a cluster away from a CNT end, for example, during Ostwald ripening, results in the creation of an open CNT end with dangling C bonds, each of which increases the energy by about 1.5 or 2.5 eV for armchair and zigzag nanotubes, respectively.[25,27] For Ostwald ripening to occur, this energy has to be regained by increasing the bulk-to-surface fraction of the larger cluster.

The energies in Figure 2 show that a set with two (3,3) CNTs attached to Ni_{30} clusters will gain approximately 6 eV by forming a set with one CNT attached to a Ni_{60} and leaving the other CNT end open. This shows that the energy gained by the formation of the larger cluster is sufficient to compensate for the creation of six dangling bonds of the open CNT. These energies are given in Table 1, which also presents energies for (6,0),

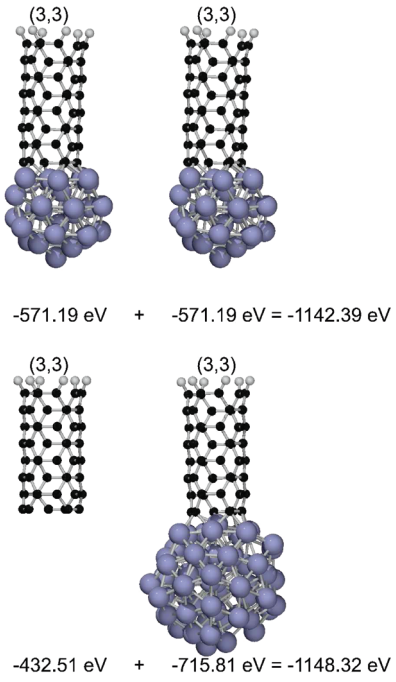

Figure 2. Structures of sets containing two (3,3) CNTs and 60 Ni atoms. The Ni atoms are distributed equally on both CNTs (top) or on only one CNT (bottom) leaving the other CNT with one open end. The total energy of each set is given as well as the energies of the individual CNT−metal systems. The difference in total energy is approximately 6 eV in favor of the set with one open CNT end and a Ni_{60} cluster attached to the other CNT.

TABLE 1. Total Energies of Sets with Two (*n*,*m*) CNTs Attached to a Total of 60 Ni Atoms[a]

	total energies of CNT−metal systems	
system	energies (eV)	E_{tot} (eV)
(3,3)-Ni_{30}, (3,3)-Ni_{30}	−571.19, −571.19	−1142.39
(3,3), (3,3)-Ni_{60}	−432.52, −715.81	−1148.32
(6,0)-Ni_{30}, (6,0)-Ni_{30}	−573.28, −573.28	−1146.57
(6,0), (6,0)-Ni_{60}	−430.20, −717.06	−1147.25
(4,4)-Ni_{30}, (4,4)-Ni_{30}	−730.07, −730.07	−1460.14
(4,4), (4,4)-Ni_{60}	−588.27, −847.07	−1462.33
(8,0)-Ni_{30}, (8,0)-Ni_{30}	−730.57, −730.57	−1461.13
(8,0), (8,0)-Ni_{60}	−582.02, −875.36	−1458.28

[a] The Ni atoms are either distributed equally on both CNTs or on only one CNT. These sets are referred to as (*n*,*m*)-Ni_{30}, (*n*,*m*)-Ni_{30} and (*n*,*m*), (*n*,*m*)-Ni_{60}, respectively. The CNT chiralities are (3,3), (6,0), (4,4), and (8,0).

(4,4), and (8,0) CNTs. It shows that, in the case of (6,0) CNTs, forming the set with a large cluster and an open CNT end will lead to an energy gain of approximately 0.7 eV, which is a significantly smaller energy gain than for the (3,3) CNT. This is a reasonable result, since the adhesion between zigzag CNTs and Ni clusters is stronger than the adhesion between armchair CNTs and Ni clusters.[24] Consequently, the energy required to separate the cluster from a zigzag CNT is higher than that required for separation from an armchair CNT (with the same number of carbon end atoms).

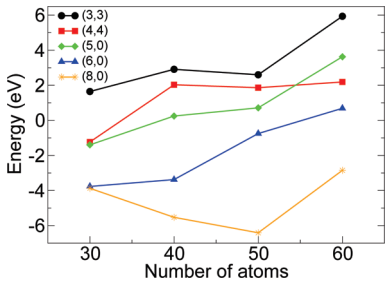

Figure 3. The relative stabilities for (3,3), (4,4), (5,0), (6,0), and (8,0) CNTs are plotted against the total number of Ni atoms. A positive relative stability indicates that it is energetically favorable to form a set with one open CNT end and all Ni atoms attached to the other CNT end compared to having an equal number of Ni atoms at each CNT end.

The formation of one large Ni_{60} cluster instead of two Ni_{30} clusters is favored by 2.2 eV for the (4,4) CNT but is disfavored by 2.8 eV for the (8,0) CNT. Again, this shows that zigzag CNTs are less prone to experience Ostwald ripening of the catalyst particles and that the formation of the Ni_{60} cluster does not provide a sufficient energy to compensate for the formation of eight dangling C bonds.

Figure 3 shows the relative energies between sets with a total number of 30, 40, 50, and 60 Ni atoms distributed either as two small clusters of the same size or as one large cluster. The CNT chiralities are (3,3), (4,4), (5,0), (6,0), and (8,0), and a positive relative energy indicates that the set with one larger cluster and one open CNT is more stable than the set with one smaller cluster at each CNT end. It is clear that even the formation of a small cluster of 30 Ni atoms is sufficient to compensate for the formation of six dangling C bonds at an open (3,3) end while at least 40 Ni atoms are needed to compensate for the creation of eight dangling bonds at the (4,4) end. The zigzag CNTs, which have stronger adhesion to the Ni cluster need at least 40, 60, and >60 Ni atoms for the (5,0), (6,0), and (8,0) CNTs to be left with an open end, respectively. The observed trends with increased stability with increased cluster size are similar to the trend for free clusters shown in Figure 1. This supports the validity of the calculation although there is a small effect of the initial configuration, most clearly seen for the 40 and 50 atom clusters attached to the (8,0) CNT.

These results, which represent the extreme case where all atoms are removed from one CNT, support the fact that Ostwald ripening may occur with clusters attached to CNTs. This may terminate the growth of parts of the initial CNT distribution. The CNTs that no longer have attached metal clusters after Ostwald ripening will not grow in length. Also, an increase in cluster size due to the Ostwald ripening may lead to solidification of the particle at the growth temperature,[28,29] which may also terminate the growth.[30] The mechanism of the growth termination lies outside the scope of this contribution.

The behavior of a mixed distribution of armchair and zigzag CNTs was analyzed by energy comparisons of

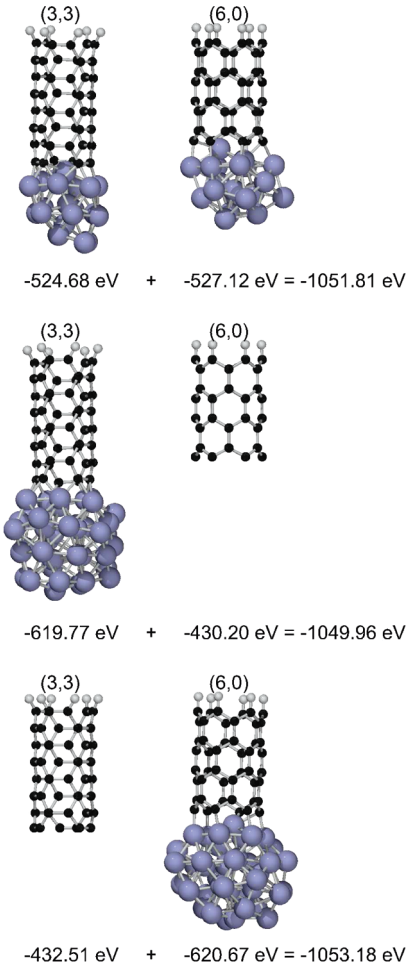

Figure 4. Sets with a (3,3) and a (6,0) CNT and a total of 40 Ni atoms distributed equally (top), on the (3,3) CNT (middle), and on the (6,0) CNT (bottom).

sets containing an armchair and a zigzag CNT with an equal number of bonds at the end, that is, (3,3) and (6,0) or (4,4) and (8,0). These CNTs were either attached to Ni clusters of the same size (top panel in Figure 4) or one CNT is attached to a large cluster and the other CNT is left with an open end (middle and bottom panels in Figure 4). A comparison of the total energies of the sets shows that it is 1.4 eV more favorable to form a larger cluster at the zigzag end, leaving the armchair CNT open, than having a smaller cluster at each CNT end. It is also seen that leaving the zigzag end open and having the larger cluster at the armchair CNT leads to an energy cost of 1.9 eV. This means that, under conditions suitable for Ostwald ripening, the cluster atoms initially attached to the armchair CNT will diffuse to the clusters attached to the zigzag CNTs. Similar results were obtained for the sets containing (4,4) and (8,0) CNTs and 60 Ni atoms, where the energy of the set with all 60 Ni atoms at the zigzag end is approximately 3 eV lower than for the set with 30 Ni atoms end which is approximately 3.6 eV lower than for the set with all Ni atoms at the armchair end.

TABLE 2. Total Energies of Sets with Two (*n*,*m*) CNTs Attached to a Total of 40 Ni Atoms[a]

	total energies of CNT−metal systems	
system	energies (eV)	E_{tot} (eV)
(3,3)-Ni_{20}, (3,3)-Ni_{20}	−524.68, −524.68	−1049.36
(3,3)-Ni_{15}, (3,3)-Ni_{25}	−501.04, −548.06	−1049.10
(6,0)-Ni_{20}, (6,0)-Ni_{20}	−527.12, −527.12	−1154.25
(6,0)-Ni_{15}, (6,0)-Ni_{25}	−503.62, −549.71	−1153.33

[a] The Ni atoms are either distributed equally on both CNTs or with 15 Ni atoms on one CNT and 25 Ni atom on the other CNT. These sets are referred to as (*n*,*m*)-Ni_{20}, (*n*,*m*)-Ni_{20} and (*n*,*m*)-Ni_{15}, (*n*,*m*)-Ni_{25}, respectively. The CNT chiralities are (3,3) and (6,0).

The requirement for Ostwald ripening of free clusters to occur is that there exists a width in the cluster size distribution. To evaluate whether this condition is sufficient for Ostwald ripening of clusters attached to CNTs, a comparison was done of the total energies between two sets, containing a total of 40 Ni atoms, distributed either as two Ni_{20} clusters or as a Ni_{15} and a Ni_{25} cluster, when attached to (3,3) and (6,0) CNTs (Table 2). The sets with an equal Ni distribution are favored by approximately 0.25 and 0.8 eV for the (3,3) and (6,0) CNTs, respectively. This means that a size distribution of width 5 atoms, centered around 20 atoms, is not sufficient to initiate Ostwald ripening of Ni clusters attached to (3,3) and (6,0) CNTs. On the contrary, Ni clusters within this size distribution will undergo ripening toward the most stable distribution, that is, when all clusters have the same size. It is important to note that this is the opposite trend that was seen for the (3,3) CNT when the comparison was made between a set containing two Ni_{20} clusters and a set containing a Ni_{40} cluster (Figure 2), while it is the same trend for the (6,0) CNT. In the first case, Ostwald ripening to the large cluster was observed while in the latter it was not observed.

The above results show that when the Ni clusters are attached to CNTs, not only is the Ostwald ripening governed by a critical size forcing clusters above this size to increase in size at the expense of the clusters below this critical size, but also the ripening process is governed by a critical factor which is a combined property of increased stability due both to cluster size and stabilization due to the adhesion to the CNT.

The comparisons between zigzag and armchair CNTs indicate that this critical factor is different for clusters attached to different CNT chiralities, even though the cluster size is the same. This can be further analyzed by studies of the Ni atomic energies. Figure 5 shows histograms of the atomic energies of the atoms in the Ni_{55} cluster attached to (5,5) and (10,0) CNTs. These systems were studied in ref 25 and have CNT-cluster adhesion energies of approximately −14.5 and −25.2 eV for the (5,5) and (10,0) CNTs, respectively. Atoms have been characterized into three categories which are

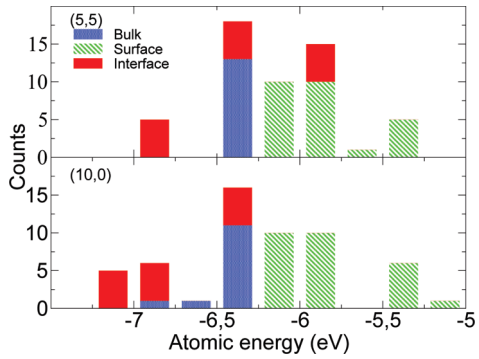

Figure 5. Histograms of the Ni atomic energies in the CNT(5,5)-Ni_{55} (top) and CNT(10,0)-Ni_{55} (bottom) systems. The cluster atoms have been separated into bulk Ni, surface Ni, and interfacial Ni. It is seen that the energies of the bulk and surface atoms are very similar for both CNT systems while the energies of the interfacial atoms are lower (higher stability) for the CNT(10,0)-Ni_{55} system.

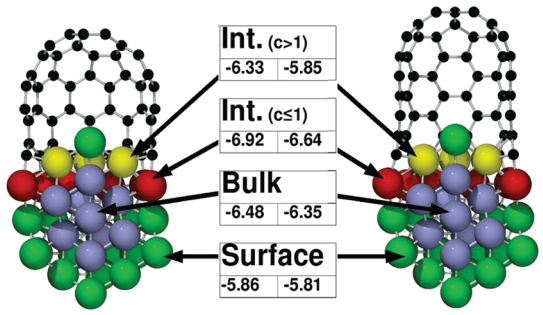

Figure 6. Ni atomic energies in systems with (10,0) (left) and (5,5) (right) CNTs attached to icosahedral Ni_{55} clusters. The average atomic energies are given for bulk Ni (blue) atoms, surface Ni (green) atoms, interfacial Ni atoms with C coordination number less than or equal to 1, (red) and interfacial Ni atoms with C coordination number greater than 1 (yellow).

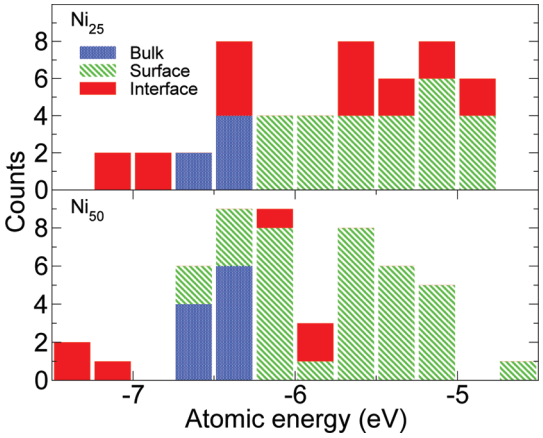

Figure 7. Histograms of the atomic energies of Ni atoms in the CNT(3,3)-Ni_{25} (top) and CNT(3,3)-Ni_{50} (bottom) systems. The atoms have been separated into bulk Ni, surface Ni, and interfacial Ni. For CNT(3,3)-Ni_{25} every atomic energy has been counted twice in order to have a total of 50 Ni atoms which makes the two histograms directly comparable. It is seen that the CNT(3,3)-Ni_{50} system has a larger number of bulk atoms and that both the surface and interfacial distributions are shifted toward lower energies and increased stability.

separately indicated in the histograms. Bulk atoms have coordination numbers $coord_{Ni-Ni} > 11$ and $coord_{Ni-C} = 0$, surface atoms have $coord_{Ni-Ni} \leq 11$ and $coord_{Ni-C} = 0$ and interfacial atoms have a coordination number $coord_{Ni-C} > 0$. It is seen that bulk atoms have approximately the same atomic energies for both systems, meaning that these are equally stable and that there is no energetic preference to form more bulk on either CNT during the course of Ostwald ripening. A similar trend is seen for surface atoms which is expected since the clusters are of the same size. The difference in the energy distributions of the interfacial atoms shows that they are more stable at the (10,0)-cluster interface than at the (5,5)-cluster interface. This means that there is a higher cost of removing atoms from the (10,0)-cluster interface and that the removal of these atoms requires a higher critical factor than the removal of atoms from the (5,5)-cluster interface. This is consistent with the results discussed above, where it was seen that a larger cluster is required to remove all atoms from a zigzag end than an armchair end. Comparison of the atomic energies also indicates that the stabilization is due to local effects at the CNT end and hence, the difference in contribution to the critical factor for armchair and zigzag is due only to this region. The results here are typical for other cluster geometries and sizes.

In Figure 6 the energies of the interfacial atoms have been divided into two groups, having coordination numbers $coord_{Ni-C} \leq 1$ and $coord_{Ni-C} > 1$. The average energies for each group are given for both systems as well as their positions on a cross section of the structures. It is seen that atoms on the interface with $coord_{Ni-C} \leq 1$ are the most stable while interfacial atoms with $coord_{Ni-C} > 1$ are more stable than surface atoms but less stable than bulk.

It is interesting to note that the lower stability of interfacial atoms with $coord_{Ni-C} > 1$ (yellow in Figure 6) compared to bulk (blue) means that atoms inside the CNT will retract from the CNT if this increases the number of bulk atoms. This conclusion was drawn in ref 23 which was based on the analysis of local energies within a tight-binding model. Although it should be stressed that the atomic energies in this contribution and the local energies reported in in ref 23 are fundamentally different properties, this supports the validity of the tight-binding results.

A comparison of the atomic energies of Ni_{25} and Ni_{50} clusters on a (3,3) CNT end, seen in Figure 7, shows that the bulk atoms are equally stable in both systems while surface and interfacial atoms in the larger cluster are slightly more stable than in the smaller cluster. This means that there will be an energy gain to drive surface atoms from the smaller cluster to the larger cluster since they are more stable irrespective of whether they are surface or bulk in the larger cluster. The consequence of this is that that smaller cluster will decrease until only interfacial atoms remain at the CNT end. For these final

interfacial atoms to be driven to the larger cluster it is necessary that they increase their stability. Calculations of the atomic energies of eight C atoms on the end of a (8,0) CNT (chosen because of the stronger adhesion between Ni and zigzag CNTs) showed that these atoms, which form a ring at the CNT end, have an atomic energy of approximately −5.6 eV which is less stable than the bulk of larger clusters; that is, the interfacial atoms will move to the larger clusters. It is also clear that the bulk-to-surface fraction is higher for the larger cluster and that the driving force of Ostwald ripening is the same for these nanoscaled clusters as for particles on the microscale. In addition, the driving force is enhanced by the increased stability of the surface atoms, and not only because the ratio of bulk/surface atoms increases.

To verify that the results reported above are valid at temperatures relevant to CNT growth DFT molecular dynamics (MD) simulations were performed for the (3,3) and (6,0) CNTs with one open end and attached to Ni_{20} and Ni_{40} clusters. The atomic starting configurations for the MD simulations were taken from the relaxed structures providing data for Table 1 but where all atoms were slightly displaced in order to provide a quick increase in the temperature. As the MD simulations were performed with lower accuracy, as described in the Methods section, a relaxation of the starting configuration was done in order to verify that the reduced accuracy did not significantly alter the trends of the calculations at 0 K. Calculations at the lower accuracy yielded relative energies of 1.64 eV for the (3,3) CNTs and −3.48 eV for the (6,0) CNTs. This is the same trend as presented in Figure 3, where the relative energies are 2.9 and −3.4 eV, respectively.

The energy comparisons at finite temperature were done in a procedure comparable to that described above but where the minimum energies are replaced by average energies with corresponding standard deviations. The data sampling was performed during a simulation time of 0.75 ps after an equilibration time of at least 1.5 ps. The relative average energies are obtained from $E_{rel} = 2 \times E_{CNT-Ni_x} - E_{CNT-Ni_{2x}} - E_{CNT}$, and the relative standard deviation of the relative average energies were calculated as the square root of the sum of squared standard deviations, that is, by the expression $\sigma_{rel} = (2 \times \sigma_{CNT-Ni_x}{}^2 + \sigma_{CNT-Ni_{2x}}{}^2 + \sigma^2_{CNT})^{1/2}$. For the (3,3) CNT the average relative energy was $E_{rel} = 2.68$ eV with the relative standard deviation $\sigma_{rel} = 1.07$ eV. The positive relative energy indicates that the set with two identical clusters is less stable than the set where all Ni atoms were part of one large cluster attached to one of the CNTs.

For the sets with (6,0) CNTs the average relative energy was $E_{rel} = -2.2$ eV with the relative standard deviation $\sigma_{rel} = 1.08$ eV. The set with two identical clusters is clearly more stable than the set with only one large cluster. Hence, conclusions based on the calculations at 0 K are also valid at this temperature. It is worth noting that the open end of the (6,0) CNT closed during the MD simulation while that of the (3,3) CNT did not. Closure of the CNT leads to a lower energy of this set which favors Ostwald ripening. Despite this, Ostwald ripening on (6,0) CNTs is not favored compared to having two smaller clusters.

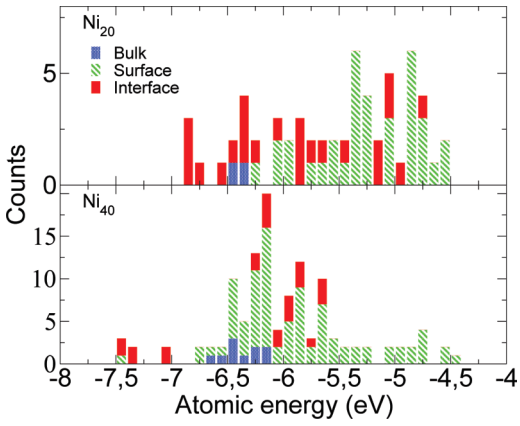

Figure 8. Histograms of the atomic energies of Ni atoms in the CNT(3,3)-Ni_{20} (top) and CNT(3,3)-Ni_{40} (bottom) systems. The histograms are based on data from three different frames from the MD simulations discussed above. The atoms have been separated into bulk Ni, surface Ni, and interfacial Ni atoms.

To elaborate further on the temperature effect on Oswald ripening, the atomic energies of Ni atoms in finite temperature configurations were calculated. This was done for three different frames of the MD simulations of the (3,3)-Ni_{20} and (3,3)-Ni_{40} systems discussed above. The histograms of these atomic energies, given in Figure 8, gives a measure of the energy cost of removing one atom from the cluster, that is, the energy lost by the system when one atom is removed from the source cluster. These calculations showed the same trend as the 0 K calculations where the atomic energies are higher for surface atoms on smaller clusters compared to surface atoms on larger clusters.

The energy cost of removing one atom can be compared with the energy gained when this atom is attached on the surface of another cluster, that is, in a start and end state diffusion process. This energy gain was approximated from the atomic energies of one Ni atom that was randomly positioned close to the metal surface in the (3,3)-Ni_{20} system. This was done for a total of 160 random positions on the three different atomic configurations of the (3,3)-Ni_{20} systems. The Ni atom was positioned between 2.1 and 2.8 Å from the nearest Ni neighbor and at least 1.7 Å away from the nearest C neighbor. The average energy of these atoms is −3.35 eV, and the most stable atoms had an atomic energy of approximately −4.45 eV, although it is reasonable to expect that more sophisticated positioning of atoms on the cluster surface may yield lower atomic energies. The lowest cost of removing an atom from a cluster surface (seen in Figure 8) is larger than the energy gained when attaching to a new cluster.

More quantitatively, the maximum energy of the surface Ni atoms of the (3,3)-Ni_{20} system is approximately −4.55 eV, while the minimum atomic energies of the randomly positioned Ni atoms are approximately −4.45 eV. By comparing the situations before and after atomic diffusion an energy difference $\Delta E \approx -0.1$ eV is obtained. To include the finite temperature, the relative probability between the two states at a temperature of 1000 K can be approximated as $P_{rel} = \exp(-\Delta E/(k_B T)) \approx 0.3$. This means that there is a significant probability, ~0.3, of removing an atom from a smaller cluster and adsorption of this atom onto another cluster. Considering that the feedstock decomposition and subsequent C addition to the cluster may be exothermic which would give even higher cluster temperatures, the relative probability may be even higher. Further, this calculation assumes a maximum dissociation barrier of the diffusing atom as it was just removed from the source cluster without any reconfiguration. If the reconfiguration was to be taken into account the dissociation barrier may be lower and thus yielding a higher relative probability between the systems. Finally, the addition of an atom to a cluster is likely to result in a reconfiguration of the target cluster with the result that the newly added atom will increase in stability shortly after the addition. The average atomic energies of the surface atoms are approximately −5.25 eV for the Ni atoms of the (3,3)-Ni_{20} system and approximately −5.85 eV for the Ni atoms of the (3,3)-Ni_{40} system. This means that the reconfiguration of the target cluster may, on average, result in an energy decrease in the order of at least 0.5 eV.

As a final remark, the difference in atomic energy between bulk atoms and surface atoms at the finite temperature is at least $\Delta E = -0.5$ eV. This gives a relative probability at 1000 K of $P_{rel} = \exp(-\Delta E/(k_B T)) \approx 0.003$; that is, it is significantly more likely to find an atom in the bulk state if possible. The temperature needed to obtain an approximately equal relative probability is around 8500 K, which is far beyond the temperatures relevant to CNT growth and well above the clusters' melting point. Hence, a very high temperature is needed to remove the driving force for Ostwald ripening, namely, the stability difference between bulk and surface atoms.

Some of the results presented here assume that the CNT has an open (unpassivated) end after Ostwald ripening. This is not expected to be the case under experimental conditions where feedstock or other medium molecules may passivate the CNT end, or where the open end may form a cap. To illustrate the effect of passivation on our results we consider the simplest reaction of medium H_2 molecules dissociating to H atoms that passivate the open CNT end. The H_2 dissociation and C−H bond energies are calculated using the same methods described above. These energy comparisons

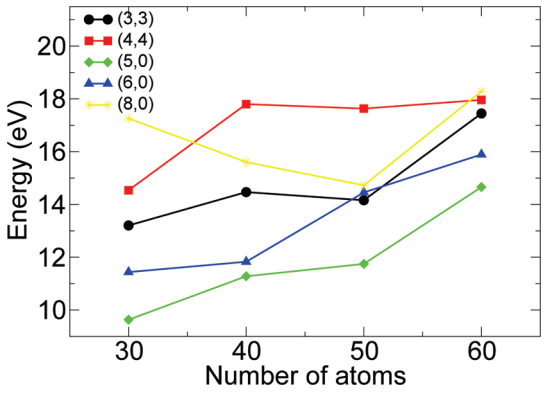

Figure 9. The relative stabilities for (3,3), (4,4), (5,0), (6,0) and (8,0) CNTs are plotted against the total number of Ni atoms. A positive relative stability indicates that it is energetically favorable to form a set with one CNT end passivated by H atoms and all Ni atoms attached to the other CNT end compared to having an equal number of Ni atoms at each CNT end and the corresponding number of H atoms in H_2 molecules.

were done for systems containing an equal amount of C, Ni, and H atoms distributed either as two Ni clusters, containing x atoms, attached to two CNTs and nH_2 molecules in the medium or as a cluster, containing $2x$ Ni atoms attached to one CNT and the other CNT passivated by the $2n$ hydrogen atoms. Similarly to the calculations presented above, the relative energies were then calculated as

$$E_{rel} = (2 \times E_{CNT-Ni_x} + n \times E_{H_2}) - E_{CNT-Ni_{2x}} - E_{CNT-2nH} \quad (4)$$

where $2n$ was chosen to be the number of C atoms at the CNT end; that is, $n = 3$ for (3,3) and (6,0), $n = 4$ for (4,4) and (8,0), and $n = 2.5$ for (5,0). The results of these calculations are seen in Figure 9. As seen, the end passivation may alter the previous results in the sense that larger CNTs may gain more energy by forming a larger cluster instead of two smaller clusters, that is, more likely to experience Ostwald ripening. The passivation of the CNT ends may also erase some of energy difference between sets with armchair and zigzag CNTs.

As discussed above (with comparison of Figure 3 and Figure 9), passivation does not change the trends of larger energy gains with Ostwald ripening, but it leads to a larger energy gain for all cluster sizes. Even smaller clusters on zigzag ends will Ostwald ripen when passivation effects are considered. However, it is important to note that the results presented above for the critical factor of Ostwald ripening (Table 1 and Figure 5, Figure 6 and Figure 7) and when narrowing of the initial cluster distribution was observed were based on calculations that did not include open CNT ends. Hence, these results are not affected by passivation. Also, under experimental conditions passivation does not completely remove the effect of dangling bonds (or C−Ni energy). That is, Ni atoms need to be partially

or fully removed from the CNT end before passivation can occur. Hence, the effect of the chirality of CNTs on Ostwald ripening will lie between the extremes of no and immediate passivation studied here.

End passivation is more complex under experimental conditions than the procedure described here and may depend on which residues are left from the feedstock decomposition, *etc.* As discussed in ref 17, the presence of water inhibits Ostwald ripening and may also affect the passivation of the CNT ends. Although many details remain to be investigated it can be concluded that ripening behavior of the metal clusters is expected to be very different in an environment containing inert gases compared to, for example, hydrogen.

CONCLUSIONS

The results in this contribution shows that the Ostwald ripening process may be responsible for the termination of growth of fractions of CNT forests and that CNTs with strong adhesion to the metal particle are more prone to survive through the course of ripening. It was also shown that the driving force of Ostwald ripening in the case of Ni clusters attached to CNTs is a combined property of increasing the bulk-to-surface fraction of the cluster and minimization of the number of dangling C bonds on the CNT ends. It is concluded that it is more appropriate to describe evolution of cluster distributions by their relation to a critical factor rather than a critical size, as in the case of free clusters. Since this critical factor is not only dependent on cluster size, it was seen that the critical factor may have an extreme point at a certain cluster size and CNT adhesion, meaning that an inverse ripening process may occur which will narrow the distribution rather than widening it. For example, it was seen that two clusters containing 15 and 25 atoms each and that are attached to (3,3) or (6,0) CNTs are less stable than when the clusters contain 20 atoms each. However, the most stable structure is when all 40 atoms are in a cluster attached to one of the CNTs. The contributions to the critical factor were seen to be local; that is, only the part of the cluster close to the CNT end contributes, while the parts of the cluster further from the CNT behave as if they were part of a free cluster.

METHOD

The DFT calculations were performed using the Vienna *ab initio* simulation package (VASP)[31] using a plane-wave basis set in combination with ultrasoft pseudopotentials (US-PP). All DFT results are from spin polarized calculations performed using the PW91[32] exchange-correlation functional. The plane-wave energy cutoff was set to 400 eV during the geometry optimizations, and a Gaussian Fermi level smearing of 0.05 eV was used for all calculations. The supercell had a size of 15 Å × 15 Å × 30 Å for the systems containing a CNT and 15 Å × 15 Å × 15 Å for systems containing only Ni. Tests with different plane-wave energy cutoffs, box sizes, and box geometries showed that these settings were sufficient to converge the total energies to less than 1 meV/atom and to allow for Γ-point sampling of *k*-space.

The geometry optimizations, performed using the conjugate gradient algorithm without any symmetry constraints, were stopped when the total energy difference between consecutive relaxation steps were less than 10^{-4} eV. This method and parameters have been successfully used in previous studies of CNT−metal systems, for example, in refs 23−25, 27, and 33.

In addition to the geometry optimizations a few molecular dynamics (MD) simulations were performed using the Verlet algorithm with a time step of 1.5 fs. During the MD simulations the plane-wave energy cutoff was set to 250 eV. The average temperature during these simulations was approximately 800 K for all systems.

The total energies presented here are relative to a reference energy defined by the pseudo-potentials. Since all conclusions are based on comparisons of energy differences between systems with an equal number of Ni and C atoms, the reference energy will be the same for both systems and will cancel in the comparison.

The input structures consist of a CNT with one end passivated by a ring of H atoms and the other end is either left open or attached to a Ni cluster. The CNT chiralities used were (3,3), (4,4), (5,0), (6,0), and (8,0), and all CNTs were attached to Ni clusters containing 15, 20, 25, 30, 40, 50, or 60 atoms. The Ni clusters were constructed by random positioning of Ni atoms within a compact cluster shape constrained by a minimum interatomic distance of 2 Å. The Ni clusters were positioned near the open CNT ends with the constraint that the distance between C and Ni atoms should not be below 1.8 Å. In addition, capped (5,5) and (10,0) CNTs attached to an icosahedral Ni_{55} cluster were studied.

For all systems two sets, with different initial Ni configuration, were relaxed. All results originate from the most stable system, that is, the system with the lowest total energy. Although limited, this procedure should decrease the effect associated with the difficulty to find relevant minimum energy structures of systems of high dimensionality. It is reasonable to believe that the difficulty in finding the relevant minimum structure will increase with increasing dimensionality, that is, with increasing number of atoms. This means that comparisons of small and large cluster systems based on the energies obtained from our calculations may favor the smaller clusters. It is therefore important to note that conclusions drawn in this contribution are based on observations of general trends rather than individual energies. This procedure is valid despite the fact that results of individual calculations may depend on the initial configuration since the trends exhibited by larger sets of computational data are not sensitive to individual results that deviate from the trend. Typically, the uncertainty of individual energy contributions are seen as deviations from the increasing cluster stability with increasing cluster size.

Acknowledgment. The authors are grateful for time allocated on the Swedish National Supercomputing facilities and for support obtained from the C3SE, NSC, and UPPMAX computing resources. Financial support was obtained from the Swedish Research Council and the Nanoparticle Platform at University of Gothenburg.

REFERENCES AND NOTES

1. Anantram, M. P.; Leonard, F. Physics of Carbon Nanotube Electronic Devices. *Rep. Prog. Phys.* **2006,** *69*, 507–561.
2. Avouris, P.; Chen, Z.; Perebeinos, V. Carbon-Based Electronics. *Nat. Nanotechnol.* **2007,** *2*, 605–615.
3. Niu, C.; Sichel, E. K.; Hoch, R.; Moy, D.; Tennent, H. High Power Electrochemical Capacitors Based on Carbon Nanotube Electrodes. *Appl. Phys. Lett.* **1997,** *70*, 1480–1482.

4. Coleman, J. N.; Kahn, U.; Gun'ko, Y. K. Mechanical Reinforcement of Polymers Using Carbon Nanotubes. *Adv. Mater.* **2006,** *18*, 689–706.
5. Moniruzzaman, M.; Winey, K. I. Polymer Nanocomposites Containing Carbon Nanotubes. *Macromolecules* **2006,** *39*, 5194–5205.
6. Kilbride, B. E.; Coleman, J. N.; Fraysse, J.; Fournet, P.; Cadek, M.; Dury, A.; Hutzler, S.; Roth, S.; Blau, W. J. Experimental Observation of Scaling Laws for Alternating Current and Direct Current Conductivity in Polymer−Carbon Nanotube Composite Thin Films. *J. Appl. Phys.* **2002,** *92*, 4024–4030.
7. Biercuk, M. J.; Llaguno, M. C.; Radosaveljevic, M.; Hyun, J. K.; Johnson, A. T.; Fischer, J. E. Carbon Nanotube Composites for Thermal Management. *Appl. Phys. Lett.* **2002,** *80*, 2767–2769.
8. Ci, L.; Suhr, J.; Pushparaj, V.; Zhang, X.; Ajayan, P. M. Continuous Carbon Nanotube Reinforced Composites. *Nano Lett.* **2008,** *8*, 2762–2766.
9. Yao, Y.; Liu, C.; Fan, S. Anisotropic Conductance of the Multiwall Carbon Nanotube Array/Silicone Elastomer Composite Film. *Nanotechnology* **2006,** *17*, 4374–4378.
10. Fan, S.; Chapline, M. G.; Franklin, N. R.; Tombler, T. W.; Cassell, A. M.; Dai, H. Self-oriented Regular Arrays of Carbon Nanotubes and their Field Emission Properties. *Science* **1999,** *283*, 512–514.
11. Chhowalla, M.; Teo, K. B. K.; Ducati, C.; Rupesinghe, N. L.; Amaratunga, G. A. J.; Ferrari, A. C.; Roy, D.; Robertson, J.; Milne, W. I. Growth Process Conditions of Vertically Aligned Carbon Nanotubes Using Plasma Enhanced Chemical Vapor Deposition. *J. Appl. Phys.* **2001,** *90*, 5308–5317.
12. Zhong, G.; Iwasaki, T.; Robertson, J.; Kawarada, H. Growth Kinetics of 0.5 cm Vertically Aligned Single-Walled Carbon Nanotubes. *J. Phys. Chem. B* **2007,** *111*, 1907–1910.
13. Hoffman, S.; Csányi, G.; Ferrari, A. C.; Payne, M. C.; Robertson, J. Surface Diffusion: The Low Activation Energy Path for Nanotube Growth. *Phys. Rev. Lett.* **2005,** *95*, 036101.
14. Bower, C.; Zhou, O.; Zhu, W.; Werder, D. J.; Jin, S. Nucleation and Growth of Carbon Nanotubes by Microwave Plasma Chemical Vapor Deposition. *Appl. Phys. Lett.* **2000,** *77*, 2767–2769.
15. Hata, K.; Futaba, D. N.; Mizuno, K.; Namai, T.; Yumura, M.; Iijima, S. Water-Assisted Highly Efficient Synthesis of Impurity-free Single-Walled Carbon Nanotubes. *Science* **2004,** *306*, 1362–1364.
16. Yoshihara, N.; Ago, H.; Tsuji, M. Chemistry of Water-Assisted Carbon Nanotube Growth over Fe-Mo/MgO Catalyst. *J. Phys. Chem. C* **2007,** *111*, 11577–11582.
17. Amama, P. B.; Pint, C. L.; McJilton, L.; Kim, S. M.; Stach, E. A.; Murray, P. T.; Hauge, R. H.; Maruyama, B. Role of Water in Super Growth of Single-Walled Carbon Nanotube Carpets. *Nano Lett.* **2009,** *9*, 44–49.
18. Kim, S. M.; Pint, C. L.; Amama, P. B.; Zakharov, D. N.; Hauge, R. H.; Maruyama, B.; Stach, E. A. Evolution in Catalyst Morphology Leads to Carbon Nanotube Growth Termination. *J. Phys. Chem. Lett.* **2010,** *1*, 918–922.
19. Amama, P. B.; Pint, C. L.; Kim, S. M.; McJilton, L.; Eyink, K. G.; Stach, E. A.; Hauge, R. H.; Maruyama, B. Influence of Alumina Type on the Evolution and Activity of Alumina-Supported Fe Catalysts in Single-Walled Carbon Nanotube Carpet Growth. *ACS Nano* **2010,** *4*, 895–904.
20. Voorhees, P. W. The Theory of Ostwald Ripening. *J. Stat. Phys.* **1985,** *38*, 231–252.
21. Kabalnov, A. S.; Shchukin, E. D. Ostwald Ripening Theory: Applications to Fluorocarbon Emulsion Stability. *Adv. Colloid Interface Sci.* **1992,** *38*, 69–97.
22. Finsy, R. On the Critical Radius in Ostwald Ripening. *Langmuir* **2004,** *20*, 2975–2976.
23. Börjesson, A.; Zhu, W.; Amara, H.; Bichara, C.; Bolton, K. Computational Studies of Metal−Carbon Nanotube Interfaces for Regrowth and Electronic Transport. *Nano Lett.* **2009,** *9*, 1117–1120.
24. Ding, F.; Larsson, P.; Larsson, J.; Ahuja, R.; Duan, H.; Rosen, A.; Bolton, K. The Importance of Strong Carbon−Metal Adhesion for Catalytic Nucleation of Single-Walled Carbon Nanotubes. *Nano Lett.* **2008,** *8*, 463–468.
25. Börjesson, A.; Bolton, K. First Principles Studies of the Effect of Nickel Carbide Catalyst Composition on Carbon Nanotube Growth. *J. Phys. Chem. C* **2010,** *114*, 18045–18050.
26. Shibuta, Y.; Maruyama, S. Bond-Order Potential for Transition Metal Carbide Cluster for the Growth Simulation of a Single-Walled Carbon Nanotube. *Comput. Mater. Sci.* **2007,** *39*, 842–848.
27. Larsson, P.; Larsson, J. A.; Ahuja, R.; Ding, F.; Yakobson, B. I.; Duan, H.; Rosén, A.; Bolton, K. Calculating Carbon Nanotube−Catalyst Adhesion Strengths. *Phys. Rev. B* **2007,** *75*, 115419.
28. Buffat, P.; Borel, J.-P. Size Effect on the Melting Temperature of Gold Particles. *Phys. Rev. A* **1976,** *13*, 2287–2298.
29. Ding, F.; Rosén, A.; Curtarolo, S.; Bolton, K. Modeling the Melting of Supported Clusters. *Appl. Phys. Lett.* **2006,** *88*, 133110.
30. Harutyunyan, A. R.; Tokune, T.; Mora, E. Liquid as a Required Catalyst Phase for Carbon Single-Walled Nanotube Growth. *Appl. Phys. Lett.* **2005,** *87*, 051919.
31. Kresse, G.; Furthmüller, J. Efficient Iterative Schemes for *ab Initio* Total-Energy Calculations Using a Plane-Wave Basis Set. *Phys. Rev. B* **1996,** *54*, 11169–11186.
32. Perdew, J. P.; Chevary, J. A.; Vosko, S. H.; Jackson, K. A.; Pederson, M. R.; Singh, D. J.; Fiolhais, C. Atoms, Molecules, Solids, and Surfaces: Applications of the Generalized Gradient Approximation for Exchange and Correlation. *Phys. Rev. B* **1992,** *46*, 6671–6687.
33. Zhu, W.; Börjesson, A.; Bolton, K. DFT and Tight Binding Monte Carlo Calculations Related to Single-Walled Carbon Nanotube Nucleation and Growth. *Carbon* **2010,** *48*, 470–478.